

Determination of the refractive indices of photonic crystal layers from anodic alumina

© M.V. Pyatnov,^{1,2} M.M. Sokolov,² I.A. Kiselev,² R.G. Bikbaev,^{1,2} P.S. Pankin,^{1,2} I.R. Volkova,^{1,3}
V.A. Gunyakov,¹ M.N. Volochaev,¹ I.I. Ryzhkov,^{2,4} S.Ya. Vetrov,^{1,2} I.V. Timofeev,^{1,2} V.F. Shabanov^{1,3}

¹ Kirensky Institute of Physics, Krasnoyarsk Scientific Center, Siberian Branch, Russian Academy of Sciences, 660036 Krasnoyarsk, Russia

² Siberian Federal University, 660041 Krasnoyarsk, Russia

³ Krasnoyarsk Scientific Center of the Siberian Branch of the Russian Academy of Sciences, 660036 Krasnoyarsk, Russia

⁴ Institute of Computational Modeling, Siberian Branch, Russian Academy of Sciences, 660036 Krasnoyarsk, Russia
e-mail: MaksPyatnov@yandex.ru

Received August 31, 2023

Revised October 29, 2023

Accepted October 29, 2023

Samples of photonic crystals with a different number of structure periods were fabricated by the method of anodizing aluminum foil. Using the angular dependence of transmission spectra, transmission electron microscopy data and numerical simulation, the refractive indices of photonic crystal layers are determined. The structure of the samples, the thickness of the layers and their porosity were determined. The theory of the effective medium in the approximations of Bruggemann, Maxwell Garnett, Monecke, Landau–Lifshitz/Looyenga, Lorentz-Lorentz, del Rio–Zimmerman–Dawe, as well as the complex refractive index is applied to determine the refractive indices of the layers. All approximations showed similar values, which indicates the possibility of using them to describe heterogeneous dielectric media.

Keywords: photonic crystal, aluminum oxide, porous material, photonic band gap, anodizing, effective refractive index.

DOI: 10.21883/0000000000

Introduction

Photonic crystals (PCs) have long established themselves as an element of microelectronics and optoelectronics devices [1]. A feature of such structures is the periodic modulation of the refraction index in space, which leads to the appearance of photonic band gaps, i.e. spectral regions in which the propagation of photons through the structure is prohibited in one, two or all three directions. PCs are used as waveguides, resonator cavities, sensors, etc. [2].

Traditional methods for obtaining PCs are: self-assembly, etching, photolithography, holographic methods, etc. [3]. Another widely used method for creating PCs is the anodizing of metal foil Al [4–7], Ti [8], Nb [9], Ta [10]. Spatial modulation of the refraction index during anodizing is achieved by changing the porosity of the oxide along the normal to the film surface.

The method makes it possible to obtain anodic PC with various parameters: porosity, thickness and number of layers, microstructure. Greater variability is achieved due to the fact that the anodizing process can be precisely controlled by changing the characteristics of the anodizing current or voltage, the temperature and concentration of the electrolyte, the purity and type of materials used, and the method of polishing the sample (chemical or

mechanical one). All this makes it possible to obtain a PC with a certain type of band gap. Compared to other specified materials, the advantages of anodic aluminum oxide lie in its mechanical, thermal and chemical stability [11–14]. Due to the possibility of flexible tuning of the band structure and strong localization of light in the sample at the frequencies of characteristic modes, anodic aluminum oxide PCs are used as optical filters [15–19], sensors [20–23], lasers and luminescence amplifiers [24,25].

As part of this work, we fabricated several PCs from anodic aluminum oxide containing different numbers of periods. The structure of PCs and their spectral properties at normal and oblique incidence were analyzed. Using the matrix transfer method, the values of the effective refraction indices of the PC layers were determined. By analyzing transmission electron microscopy (TEM) images of PCs, the porosity of their layers was determined. Using several different effective medium approximations, the effective refraction indices of the PC layers were obtained.

1. Specimens and experimental methods

To obtain PC, aluminum foil with a purity of 99.99% and a thickness of 500 μm was used. Specimens were

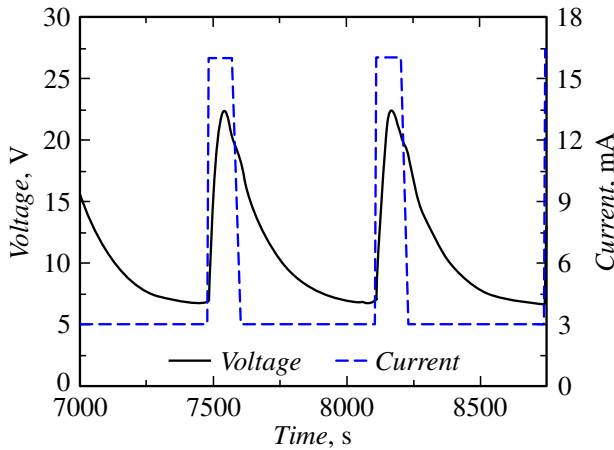


Figure 1. Dependence of the current applied to the specimen and the recorded voltage versus time in the range from 7000 to 8750 s.

degraded in isopropyl alcohol and then in ethanol. Before anodizing, electrochemical polishing of aluminum was carried out in a solution of chromic anhydride (185 g/l) and orthophosphoric acid (1480 g/l) at $T = 80^\circ\text{C}$ and current density $j = 1.0\text{ A/cm}^2$ until a mirror finish was obtained. The process of anodizing aluminum foil was carried out in a two-electrode electrochemical cell in a 1.0 M solution H_2SO_4 in the area limited by the sealing ring. The anodizing area was $S = 7.07\text{ cm}^2$. The electrolyte temperature during anodization was maintained at the level $2 \pm 1^\circ\text{C}$, while the electrolyte was stirred using a stirrer. The current profile was specified as a rectangular signal [26]. The current density was switched from $j_1 = 0.41\text{ mA/cm}^2$ to $j_2 = 2.27\text{ mA/cm}^2$ during one stage. The time duration of each stage was determined by the flow time of a charge of magnitude Q . First stage charge $Q_1 = 1.56\text{ C}$. At each subsequent stage, the charge was reduced by 0.1%, in order to compensate for the effect of chemical etching of the upper porous oxide layers in the acid electrolyte [26]. The time of the first stage with current strength $I_1 = 2.9\text{ mA}$ was 538 s, the second stage with current strength $I_2 = 16.05\text{ mA}$ —97 s. Fig. 1 shows the current parameters supported for specimen acquisition. Within one cycle, the voltage varied from 6.7 to 22 V.

Several specimens were grown with different numbers of periods N equal to 20, 30, 50, 90. After anodization, the porous oxide films were repeatedly washed in deionized water and air dried. The residual aluminum resultant product was etched off in an aqueous solution of copper chloride (0.25 M) and hydrochloric acid (5 vol.%).

The morphology of porous anodic alumina PCs was examined using an HT7700 transmission electron microscope (Hitachi). The spectral properties of the specimens were analyzed using an Ocean FX UV-VIS spectrometer in the range of 500–800 nm at normal and angular incidence.

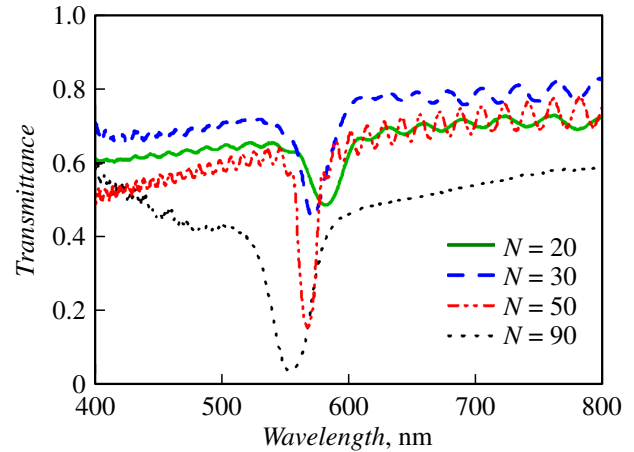


Figure 2. Measured transmission spectra of PCs from anodic aluminum oxide with different numbers of periods N .

2. Results and discussion

2.1. Angular dependences of transmission spectra

Fig. 2 shows the measured transmission spectra of the obtained samples with different numbers of periods N at normal light incidence. A pronounced dip is observed in the spectra, corresponding to the photonic band gap. Increase in the number of periods leads not only to a decrease in the transmittance at wavelengths corresponding to the stop-band, but also to a shift of the transmittance minimum to the short-wavelength region [27]. This phenomenon is due to chemical etching of the porous structure of the anodic PC in an acidic electrolyte, which leads to greater porosity of samples with large N due to the longer time required for their synthesis. As porosity increases, the effective refractive index of PC layers decreases [28], causing a blue shift of the photonic band gap to occur [29]. When the refractive indices of the PC $n_1 \approx n_2$ layers are close, the spectral position of the photonic band gap satisfies the Bragg-Snell law [30]:

$$m\lambda = 2d\sqrt{n_{\text{eff}}^2 - n_{\text{air}}^2 \sin^2 \theta}, \quad (1)$$

where λ is wavelength of the band gap center, m is band order, d is structure period, θ is angle of incidence, n_{eff} is effective refraction index of the PC, n_{air} is refraction index of the environment.

The effective refraction index of the PC and the refraction indices of the n_1 and n_2 layers are related to each other and

$$n_{\text{eff}}^2 = \frac{d_1}{d_1 + d_2} n_1^2 + \frac{d_2}{d_1 + d_2} n_2^2. \quad (2)$$

Relation (1) is a special case of a more general formula expressing the Bragg-Snell law [31]:

$$\frac{\lambda}{2} m = d_1 \sqrt{n_1^2 - n_{\text{air}}^2 \sin^2 \theta} + d_2 \sqrt{n_2^2 - n_{\text{air}}^2 \sin^2 \theta}. \quad (3)$$

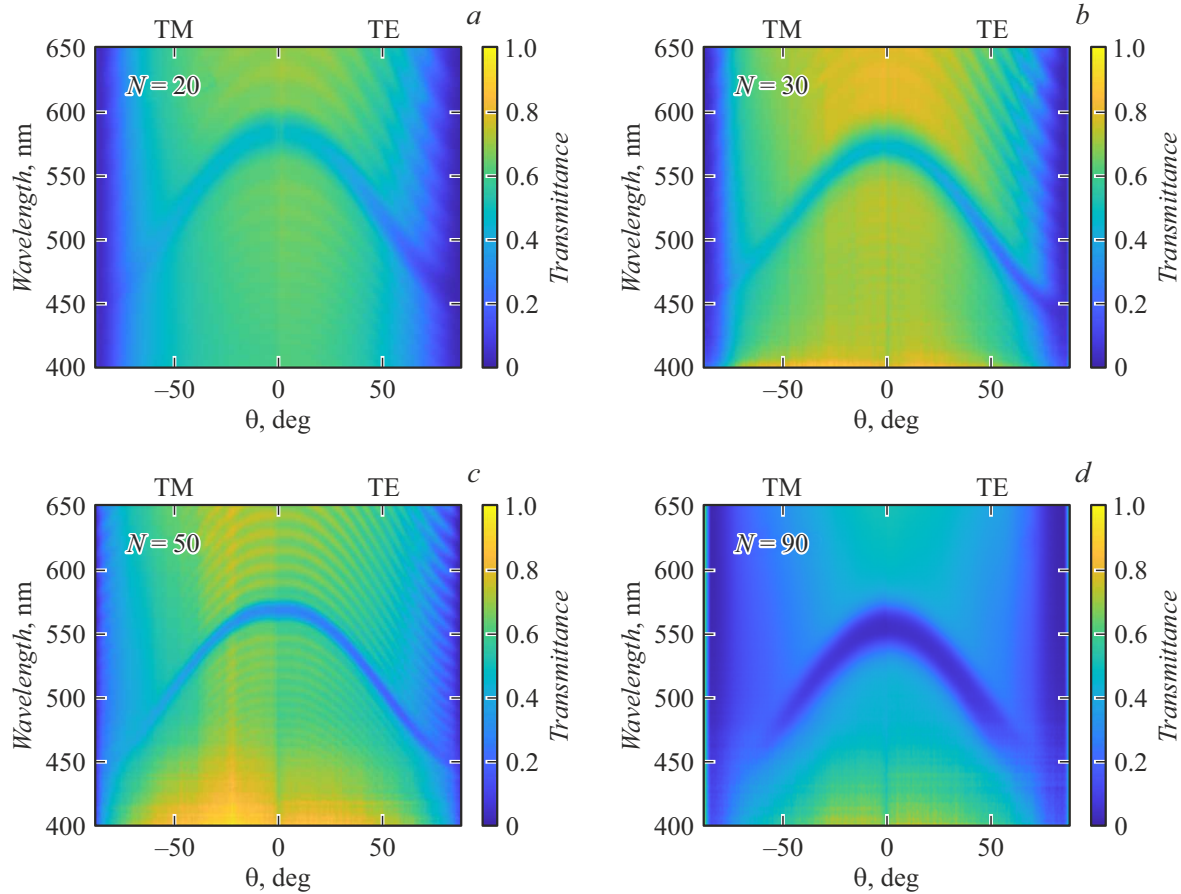


Figure 3. Measured angular dependences of the transmission spectra of photonic crystals from anodic aluminum oxide with different numbers of periods N . Positive angle values correspond to THE linear polarization of the incident light, negative angle values correspond to TM polarization of the incident light. $N = 20$ (a), 30 (b), 50 (c), 90 (d).

The band gap $\Delta\lambda$ and λ are related to the refraction indices of the PC layers n_1 and n_2 by the relation [32]:

$$\frac{\Delta\lambda}{\lambda} = \frac{4}{\pi m} \frac{|n_1 - n_2|}{n_1 + n_2}. \quad (4)$$

Fig. 3 shows the measured angular dependence of the transmission spectrum of manufactured PC samples with different numbers of structure periods. Using relations (3) and (4), the values of the PC periods and their effective refraction indices were calculated (Table 1). The obtained values of n_{eff} are close to those known from the literature [27,33].

Fig.4 shows the angular dependence of the transmission spectra of a sample with $N = 50$ calculated by the transfer matrix method and the parameters corresponding to Table 1 (3rd row). The imaginary part of the refraction indices was taken as $0.018i$ for both layers. The simulation did not take into account the dispersion of PC materials and specimen heterogeneity. It should be noted that over time, degradation of the specimens is observed, which is expressed in a decrease in the transmission value in the center of the stopband, but not in a change in its position. The calculated

Table 1. The thicknesses of the layers d_1 and d_2 , their refractive indices n_1, n_2 , found from the angular dependences of the transmission spectra using relations (3) and (4) and the effective refractive indices of PC n_{eff} , according to (2), for samples with different numbers of periods N

N	d_1 , nm	d_2 , nm	n_1	n_2	n_{eff}
20	83	89	1.65	1.73	1.69
30	114	68	1.59	1.52	1.56
50	86	94	1.54	1.60	1.57
90	107	59	1.54	1.46	1.51

spectrum gives qualitative agreement with the measured one, compare to Fig. 3, c.

2.2. TEM data

During crystal growth, pore branching occurs (Fig. 5). According to TEM images, the resulting specimen has a layered structure, high-porosity layers alternate with low-porosity ones, due to which a periodic modulation of the refraction index is created. It is known that voltage, and not

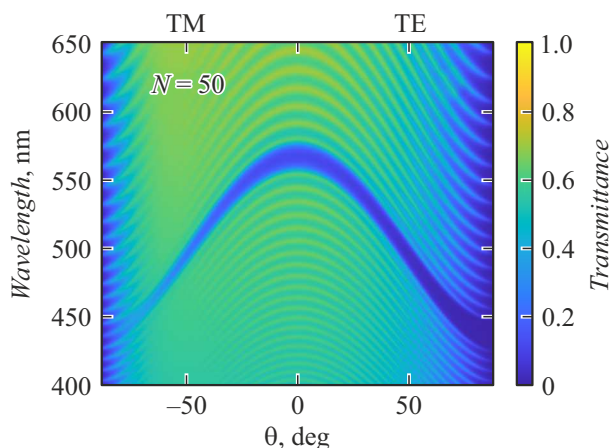


Figure 4. Calculated angular dependence of the transmission spectra of the sample with $N = 50$. FC parameters: $d_1 = 86$ nm, $n_1 = 1.54 + 0.018i$, $d_2 = 94$ nm, $n_2 = 1.6 + 0.018i$.

Table 2. Comparison of effective refractive indices of n_1 and n_2 for PC layers for different effective medium methods

Effective medium method	n_1	n_2
Bruggeman	1.56	1.48
Maxwell Garnett	1.57	1.49
Landau–Lifshitz/Loeng	1.56	1.48
Monecke	1.56	1.48
Lorenz–Lorenz	1.53	1.44
dRZW	1.52	1.44
Complex index of refraction	1.57	1.49

current density, is the structure control parameter during cyclic anodization [27].

Determination of layer thicknesses and calculation of PC porosity was performed by graphical data analysis using the open source software ImageJ [33]. Its operating principle is based on analyzing the contrast of shades of gray in the image. The ratio of the number of pixels whose color lies within a certain interval to the total number of pixels in the image gives the desired porosity. Using TEM images of PCs with $N = 50$, the values of the thicknesses d_1 and d_2 and the porosities of the f layers were obtained, which turned out to be equal to $d_1 = (95 \pm 10)$ nm, $f_1 = (26 \pm 5)\%$ for the high-porosity layer and $d_2 = (110 \pm 10)$ nm, $f_2 = (36 \pm 5)\%$ for the low-porosity one. Note that the value of the structure period $Id = d_1 + d_2 = (205 \pm 10)$ nm turned out to be greater than the value obtained from the angular dependence of the transmission spectra $d = 180$ nm. The reason for this may lie in the significant curvature of the pores as the crystal grows during the anodizing process, as well as in the error of the electron microscope, which is about 10%.

There are various methods for describing the optical properties of photonic crystals based on the effective

medium approximation [34], including the Bruggeman approach (5) [35], Maxwell-Garnett (6) [36,37], Landau–Lifshitz/Ljeng (7) [38], Monecke (8) [39,40], Lorenz–Lorenz (9) [41], del Rio-Zimmerman-Dave dRZW (10) [42], complex refractive index method (11). Each of the theories describes the effective dielectric constant of a heterogeneous two-component medium containing inclusions of various shapes and volume fractions of components.

Using the obtained porosity values for a specimen containing $N = 50$ periods, the values of the effective refractive indices of the PC layers were calculated (Table 2).

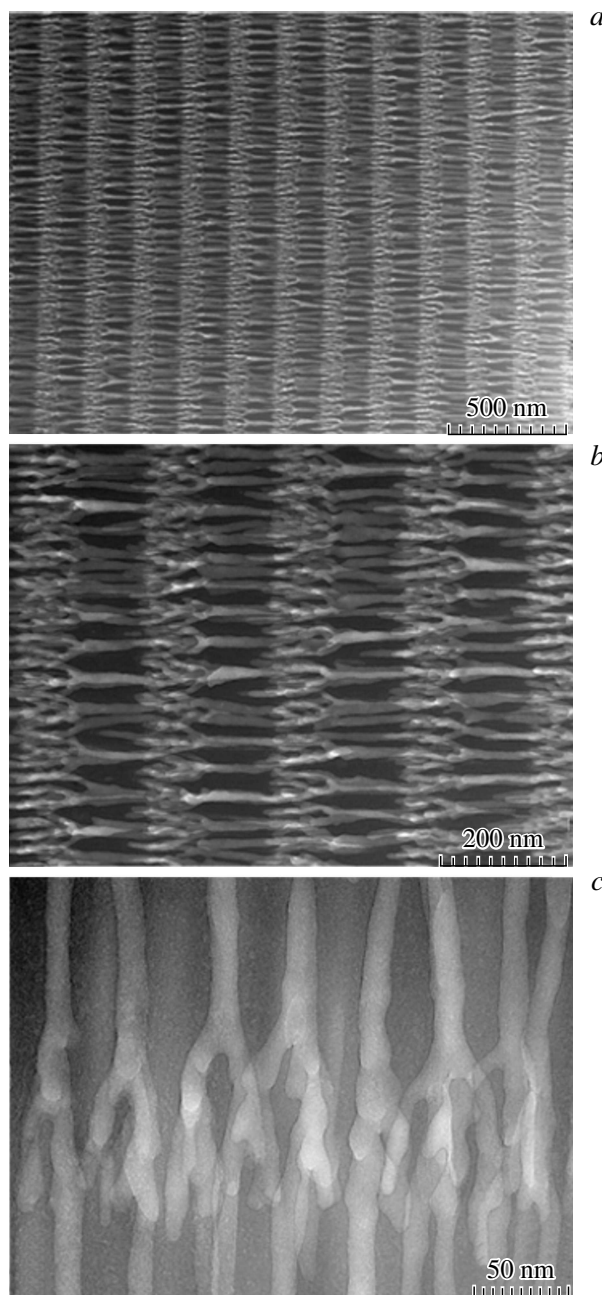


Figure 5. TEM images of the cross section of a PC with the number of periods $N = 50$ (a). Images of the specimen at low (a) medium (b) and high (c) magnification. Pores and aluminum oxide are shown in light gray and dark gray, respectively.

$n_m = 1.77$ for Al_2O_3 and $n_p = 1$ for air were taken as refraction indices of media materials.

$$f \left(\frac{n_p^2 - n^2}{n_p^2 + 2n^2} \right) + (1 - f) \left(\frac{n_m^2 - n^2}{n_m^2 + 2n^2} \right) = 0, \quad (5)$$

$$n = n_m \sqrt{\frac{f}{\frac{1-f}{3} + \frac{n_m^2}{(n_p^2 - n_m^2)}}}, \quad (6)$$

$$n = (fn_p^{2/3} + (1-f)n_m^{2/3})^{3/2}, \quad (7)$$

$$n = \sqrt{\frac{(2fn_p^2 + (1-f)n_m^2)^2 + (n_p n_m)^2}{(1+f)n_p^2 + (2-f)n_m^2}}, \quad (8)$$

$$n = \sqrt{\frac{2 \left(f \frac{(n_p^2-1)}{n_p^2+2} + (1-f) \frac{(n_m^2-1)}{n_m^2+2} \right) + 1}{1 - \left(f \frac{(n_p^2-1)}{n_p^2+2} + (1-f) \frac{(n_m^2-1)}{n_m^2+2} \right)}}, \quad (9)$$

$$n = n_m \frac{1 + f \left(\sqrt{\frac{n_p}{n_m}} - 1 \right)}{1 + f \left(\sqrt{\frac{n_p}{n_m}} + 1 \right)}, \quad (10)$$

$$n = fn_p + (1-f)n_m. \quad (11)$$

All approaches used give similar values, differing in the second sign, which generally indicates the good applicability of the effective medium method when considering dielectric heterogeneous media, which include anodic aluminum oxide PCs. At the same time, it should be noted that each of the effective medium formulas has its own limitations of applicability. Thus, the Maxwell-Garnett formula is derived assuming a low concentration of one of the components of the nanocomposite. Bruggeman's formula, on the contrary, assumes close concentrations of components. Both mentioned formulas are derived in the approximation of a composite that is unbounded in space, therefore their application to thin layers of a photonic crystal introduces an additional error due to the fact that the Lorentz sphere surrounding the point with the desired refraction index extends beyond the boundaries of the homogeneous layer. The largest deviation is observed for the dRZW method, which is based on the Keller reciprocity theorem for the effective conductivity of a composite material [43].

Conclusion

Thus, a series of aluminum oxide photonic crystal specimens were fabricated using a rectangular profile with temporal dynamics of the anode current. The influence of the number of periods of the structure on the spectral properties of the specimens was studied. Using the angular dependence of the PC and TEM transmission spectra of the manufactured specimens, their structure, layer thicknesses and porosity were determined. To find the refraction indices of crystal layers, the effective medium theory was used in the Bruggeman, Maxwell-Garnett, Moneck, Landau-Livshitz/Loeng, Lorenz-Lorenz, and dRZW approximations.

Numerical modeling of the transmission spectra of PCs was performed using the transmission spectra. The listed approximations showed close values, which indicates the possibility of their use for describing heterogeneous dielectric media.

Funding

The research was supported by a grant from the Russian Science Foundation and Krasnoyarsk Regional Science Foundation, № 22-22-20078, <https://rscf.ru/project/22-22-20078/>.

Conflict of interest

The authors declare that they have no conflict of interest.

References

- [1] J.D. Joannopoulos, P.R. Villeneuve, Sh. Fan. *Solid State Commun.*, **102** (2-3), 165 (1997). DOI: 10.1016/S0038-1098(96)00716-8
- [2] X. Lv, B. Zhong, Y. Huang, Z. Xing, H. Wang, W. Guo, X. Chang, Z. Zhang. *Chin. J. Mech. Eng.*, **36**, 39 (2023). DOI: 10.1186/s10033-023-00836-2
- [3] A.A. Yeliseyev, A.V. Lukashin. *Funktsional'nyye nanomaterialy* (Fizmatlit, M., 2010) (in Russian)
- [4] C.S. Law, S.Y. Lim, A.D. Abell, N.H. Voelcker, A. Santos. *Nanomaterials*, **8** (10), 788 (2018). DOI: 10.3390/nano8100788
- [5] G. Shang, D. Bi, V.S. Gorelik, G. Fei, L. Zhang. *Mat. Tod. Comm.*, **34**, 105052 (2023). DOI: 10.1016/j.mtcomm.2022.105052
- [6] G.D. Sulka, K. Hnida. *Nanotechnology*, **23**, 075303 (2012).
- [7] S.E. Kushnir, T.Y. Pchelyakova, K.S. Napolskii. *J. Mater. Chem. C*, **6**, 12192 (2018). DOI: 10.1039/C8TC04246B
- [8] P. Roy, S. Berger, P. Schmuki. *Angewandte Chemie International Edition*, **50** (13), 2904 (2011). DOI: 10.1002/anie.201001374
- [9] A. Mozalev, R.M. Vázquez, C. Bittencourt, D. Cossement, F. Gispert-Guirado, E. Llobet, H. Habazaki. *J. Mater. Chem. C*, **2**, 4847 (2014). DOI: 10.1039/C4TC00349G
- [10] I. Sieber, H. Hildebrand, A. Friedrich, P. Schmuki. *J. Electroceram.*, **16** (1), 35 (2006). DOI: 10.1007/s10832-006-4351-7
- [11] K.V. Chernyakova, E.N. Muratova, I.A. Vrublevsky, N.V. Lushpa. *J. Phys.: Conf. Ser.*, **2086**, 012025 (2021). DOI: 10.1088/1742-6596/2086/1/012025
- [12] Y. Suzuki, K. Kawahara, T. Kikuchi, R.O. Suzuki, S. Natsui. *J. Electrochem. Soc.*, **166**, C261 (2019). DOI: 10.1149/2.0221912jes
- [13] T. Shimizu, K. Matsuura, H. Furue, K. Matsuzak. *J. Eur. Ceram. Soc.*, **33** (15–16), 3429 (2013). DOI: 10.1016/j.jeurceramsoc.2013.07.001
- [14] M. Sarraf, B. Nasiri-Tabrizi, A. Dabbagh, W.J. Basirun, N.L. Sukiman. *Ceram. Int.*, **46** (6), 7306 (2020). DOI: 10.1016/j.ceramint.2019.11.227
- [15] G.L. Shang, G.T. Fei, Y. Zhang, P. Yan, S.H. Xu, H.M. Ouyang, L. De Zhang. *Sci. Rep.*, **4** (1), 3601 (2014). DOI: 10.1038/srep03601

- [16] A. Santos, C.S. Law, D.W.C. Lei, T. Pereira, D. Losic. *Nanoscale*, **8** (43), 18360 (2016).
- [17] C.S. Law, Sukarno, A. Santos. *Nanoscale*, **9** (22), 7541 (2017). DOI: 10.1039/C7NR02115A
- [18] G. Macias, J. Ferre-Borrull, J. Pallares, L.F. Marsal. *Nanoscale Res. Lett.*, **9** (1), 315 (2014). DOI: 10.1186/1556-276X-9-315
- [19] A.R. Gómez, L.K. Acosta, J. Ferré-Borrull, A. Santos, L.F. Marsal. *ACS Appl. Nano Mat.*, **6** (7), 5274 (2023). DOI: 10.1021/acsanm.2c05356
- [20] Y. Li, C. Yan, X. Chen, Y. Lei, B.-C. Ye. *Sensor, Actuat. B-Chem.*, **350**, 130835 (2022). DOI: 10.1016/j.snb.2021.130835
- [21] I. Garrido-Cano, L. Pla, S. Santiago-Felipe, S. Simon, B. Ortega, B. Bermejo, A. Lluch, J.M. Cejalvo, P. Eroles, R. Martínez-Manez. *ACS Sens.*, **6** (3), 1022 (2021). DOI: 10.1021/acssensors.0c02222
- [22] U. Malinovskis, A. Dutovs, R. Poplausks, D. Jevdokimovs, O. Graniel, M. Bechelany, I. Muiznieks, D. Erts, J. Prikulis. *Coatings*, **11** (7), 756 (2021). DOI: 10.3390/coatings11070756
- [23] M. Ashurov, V. Gorelik, K. Napolskii, S. Klimonsky. *Phot. Sens.*, **10**, 147 (2020). <https://doi.org/10.1007/s13320-019-0569-2>
- [24] H. Masuda, M. Yamada, F. Matsumoto, S. Yokoyama, S. Mashiko, M. Nakao, K. Nishio. *Adv. Mater.*, **18** (2), 213 (2006). DOI: 10.1002/adma.200401940
- [25] W. Yang, B. Wang, A. Sun, J. Liu, G. Xu. *Mater. Lett.*, **178**, 197 (2016). DOI: 10.1016/j.matlet.2016.05.001
- [26] L. Yisen, C. Yi, L. Zhiyuan, H. Xing, L. Yi. *Electr. Comm.*, **13**, 1336 (2011). DOI: 10.1016/j.elecom.2011.08.008
- [27] S.E. Kushnir, K.S. Napolskii. *Mat. Des.*, **144**, 140–150 (2018). DOI: 10.1016/j.matdes.2018.02.012
- [28] T.C. Choy. *Effective Medium Theory: Principles and Applications* (Clarendon Press, Oxford, 1999)
- [29] A. Santos, V.S. Balderrama, M. Alba, P. Formentín, J. Ferre-Borrull, J. Pallarés, L.F. Marsal. *Adv. Mater.*, **24** (8), 1050 (2012). DOI: 10.1002/adma.201104490
- [30] V.S. Gorelik, M.M. Yashin, D. Bi, G. Tao Fei. *Opt. Spectrosc.*, **124**, 171 (2018) (in Russian). DOI: 10.21883/OS.2018.02.45519.177-17
- [31] A. Yariv, P. Yukh. *Opticheskiye volny v kristallakh*, trans. from English Mir, M., (1987),
- [32] A. Hierro-Rodriguez, P. Rocha-Rodrigues, F. Valdés-Bango, J.M. Alameda, P.A.S. Jorge, J.L. Santos, J.P. Araujo, J.M. Teixeira, A. Guerreiro. *J. Phys. D: Appl. Phys.*, **48**, 455105 (2015). DOI: 10.1088/0022-3727/48/45/455105
- [33] Electronic source. Available at: <https://imagej.nih.gov/ij/index.html>
- [34] L.A. Apresyan, D.V. Vlasov, D.A. Zadorin, V.I. Krasovsky. *ZhTF* **87**, 10 (2017) (in Russian). DOI: 10.21883/JTF.2017.01.44011.1841
- [35] D.A. Bruggeman. *Ann. Phys.*, **24**, 636 (1935).
- [36] J.C. Maxwell-Garnett. *Phil. Trans. R. Soc. Lond.*, **203**, 385 (1904).
- [37] S.Ya. Vetrov, A.Yu. Avdeeva, M.V. Pyatnov, I.V. Timofeev. *Komp. Opt.*, **44** (3), 319 (2020). DOI: 10.18287/2412-6179-CO-637
- [38] J. Monecke. *J. Phys: Condens. Matter.*, **6**, 907 (1994). DOI: 10.1088/0953-8984/6/4/010
- [39] L.D. Landau, E.M. Lifshits. *Elektrodinamika sploshnykh sred* (Nauka, M., 2005) (in Russian)
- [10] H. Looyenga. *Physica*, **31** (3), 401 (1965). DOI: 10.1016/0031-8914(65)90045-5
- [41] B. Ersfeld, B. Felderhof. *Phys. Rev. E*, **57**, 1118 (1998). DOI: 10.1103/PhysRevE.57.1118
- [42] D. Estrada-Wiese, J.A. del Rio. *Rev. Mex. Fís.*, **64**, 72 (2018). DOI: 10.31349/RevMexFis.64.72
- [43] J.A. del Rio, R.W. Zimmerman, R.A. Dawe. *Sol. St. Comm.*, **106**, 183 (1998). DOI: 10.1016/S0038-1098(98)00051-9

Translated by V.Prokhorov